

Self-Organizing Distributed Inter-Cell Beam Coordination in Cellular Networks with Best Effort Traffic

Gerhard Wunder, Martin Kasparick, Alexander Stolyar, Harish Viswanathan

► **To cite this version:**

Gerhard Wunder, Martin Kasparick, Alexander Stolyar, Harish Viswanathan. Self-Organizing Distributed Inter-Cell Beam Coordination in Cellular Networks with Best Effort Traffic. WiOpt'10: Modeling and Optimization in Mobile, Ad Hoc, and Wireless Networks, May 2010, Avignon, France. pp.130-137, 2010. <inria-00501495>

HAL Id: inria-00501495

<https://hal.inria.fr/inria-00501495>

Submitted on 12 Jul 2010

HAL is a multi-disciplinary open access archive for the deposit and dissemination of scientific research documents, whether they are published or not. The documents may come from teaching and research institutions in France or abroad, or from public or private research centers.

L'archive ouverte pluridisciplinaire **HAL**, est destinée au dépôt et à la diffusion de documents scientifiques de niveau recherche, publiés ou non, émanant des établissements d'enseignement et de recherche français ou étrangers, des laboratoires publics ou privés.

Self-Organizing Distributed Inter-Cell Beam Coordination in Cellular Networks with Best Effort Traffic

G. Wunder, M. Kasparick
Fraunhofer MCI, Heinrich-Hertz-Institut

A. Stolyar and H. Viswanathan
Alcatel-Lucent Bell Labs, MH

Abstract—Interference reduction, cooperation and the performance of cell-edge users are important issues in next generation cellular systems. Based on previous works for single-input single-output (SISO) systems, we propose a novel interference reducing self-organizing coordination scheme for a multi antenna OFDM system with space division multiple access (SDMA). The proposed Virtual Subband Algorithm (VSA) tries to maximize the overall network utility by adjusting transmit powers on a per beam granularity and leads to a soft fractional frequency reuse. It uses only small additional information exchange between sectors and infrequent additional long-term feedback. Although reducing interference, VSA follows a completely new approach by having all beams switched-on all the time. Simulations show that in static settings compared to a non-cooperative, highly opportunistic, greedy scheduling scheme, VSA achieves significant gains both in the performance of cell-edge users and in the overall system performance, defined in this paper as the geometric average of user throughputs. Moreover it is shown that cell-edge users benefit even in fast-fading cases, although a gain in system-wide performance cannot be guaranteed.

I. INTRODUCTION

Cooperation and coordination of base stations are heavily discussed for *3GPP LTE Advanced* systems due to their potential to boost the capacity of today's cellular systems. However, with practical feedback and backhaul link capacity constraints, it is actually quite hard to obtain a big chunk of the promised gain. The situation is a bit different if cell edge users are considered, whose performance has become an important figure of merit in cellular systems. In order to increase such users' performance already simple rules for co-channel scheduling are helpful. Altogether, achieving both large capacity gain and improving the performance of cell edge users in combination with limited feedback capacity is indeed a major challenge within *LTE Advanced* research.

The general field has been addressed by many authors, see for example [1; 2; 3] and references within. The authors in [2; 4] focus on zeroforcing beamforming with perfect channel state information at the transmitter. Other recent papers also include limited feedback. In [5] the authors propose a limited feedback strategy where cooperation is restricted to sharing only the CSI of active users among base stations.

In this paper, we follow the general path outlined in [6] where power control and scheduling is employed on a suitably designed virtual model to capture the long-term interference situation in the network. Specifically, we propose a new coordination scheme for an *LTE* system equipped with multiple

antennas performing spatial beamforming, as opposed to [6] where the SISO case is investigated.

Our scheme has the following ingredients: as depicted schematically in Fig. 1, we work with a grid of fixed beams which are always “turned on” in a sense that in every slot a user is allocated to it with a fraction of the available power determined by the underlying power control scheme. Naturally, without power control a mobile terminal suffers from high interference from neighbouring beams and from beams of adjacent sectors. This interference is minimized using a power control scheme which adjusts transmit powers per beam and subband over time. This so-called Virtual Subband Algorithm (VSA) is based on a (not necessarily very frequent) message exchange between sector controllers which roughly are an estimate of the system utility's sensitivity to power changes on particular beams.

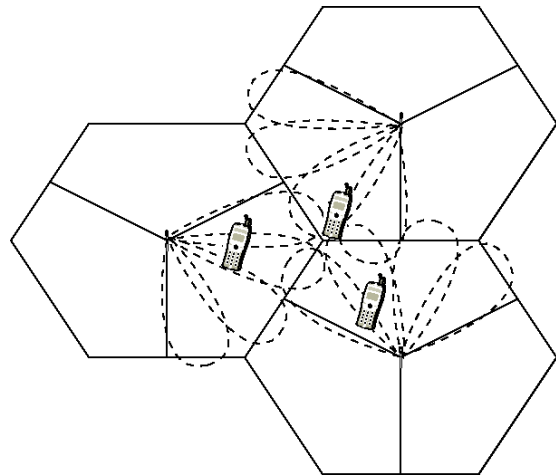


Fig. 1. System scheme using a grid of four always switched-on beams.

The overall procedure has some very striking advantages: first our scheduling algorithm automatically leads to a soft frequency and spatial reuse in the network, meaning that powers are assigned to subbands and beams such that interference is reduced. No action is required by the network operator; by contrast the network operating point can be smoothly adjusted by changing utilities on the fly.

Also important is the following observation: due to always “turned on” beams, the interference situation becomes predictable at the mobile terminal which in effect renders the

transmission much more robust with regard to limited feedback. In fact, if transmit powers and channels are known, SINRs at mobile terminals can be exactly predicted in advance, since there is no uncertainty due to scheduling.

To support our findings we will present extensive simulation results, comparing the performance of VSA to a standard non-cooperative scheduling scheme without power adaption based on a fixed minimum beam distance and a greedy user choice ([7]), which we will subsequently refer to as Greedy Beam Distance (GBD).

A. Notation

We consider the LTE downlink of a cellular 3-sectorized network comprising M sectors $m \in \{1, \dots, M\}$. Moreover we have in total I users in the network, where $I = \sum_m I_m$ and I_m being the number of users $i \in \{1, \dots, I_m\}$ served by sector m .

The time is divided into time slots $t = 1, 2, 3, \dots$, called Transmission Time Intervals (TTI) each comprising a fixed number of OFDM symbols. The total bandwidth consists of a number of subcarriers which are grouped into J subbands $j \in \{1, \dots, J\}$ called physical resource blocks (PRBs).

Each base station is equipped with N_{tx} transmit antennas, each user has N_{rx} receive antennas (in this paper we assume $N_{tx} = 4$ and $N_{rx} = 1$) forming in the sector a fixed set of beamforming vectors (shortly beams) $u \in \mathbb{C}^{N_{tx}}$ taken from a codebook $\mathcal{C}_N := \{u_1, \dots, u_N\}$ with N elements $b \in \{1, \dots, N\}$ known to everybody. $h_{ij}^m(t) \in \mathbb{C}^{N_{tx}}$ is the vector of instantaneous complex channel gains from base station m to user i in PRB j ; $\langle h_{ij}^m(t), u \rangle$ denotes the scalar product of beam u and channel $h_{ij}^m(t)$. The noise figure at the mobile terminal is denoted as σ^2 . Channel State Information (CSI) (channel quality CQI and spatial direction information CDI) is delivered by each mobile terminal to the base station using an uplink feedback channel with limited rate.

In the described setting, a potential resource to be used by user i in sector m is a beam b on PRB j , with a power value in TTI t of $P_{jb}^m(t)$. The usage of these resources is controlled by a *sector controller* in each sector.

B. General Concept

The task of all sector controllers can be outlined as to find suitable utilization times, power and rate allocations for the users in the sectors using a reasonably low rate feedback channel and infrequent message exchange across sectors. We follow a three stage approach to this problem:

First, we manipulate the system's operating point by formulating a proper network utility problem, that is

$$\max \sum_{m=1}^M \sum_{i=1}^{I_m} U^m(\bar{X}_i^m) \quad (1)$$

where U^m is a smooth concave utility of average user rates \bar{X}_i^m in sector m collected in the vector $\bar{X}^m = (\bar{X}_1^m, \dots, \bar{X}_{I_m}^m) \in \mathbb{R}_+^{I_m}$. A system operating point is a set of powers assigned to each beam-PRB pair.

Second, a standard gradient scheduler (see e.g. [8]) is applied in each sector to solve problem (1) over time. We will focus on this in detail in the next section (I-C).

Third, the main invention in this paper is a sophisticated virtual model mimicking the complicated interference situation across sectors in the real world that is typically not easy to describe. In this virtual model powers per beam and PRB serve as long-term control parameters which are adjusted according to the virtual model. Hence, we consider the optimization process of the network solely as a power control problem where the challenge is to describe how control powers affect average rates given only locally available information.

It is worth noting that short-term and long-term rates can be very different which nevertheless still makes sense in the virtual model as it is only a representative model for the interference coupling. Before we describe the actual Virtual Subband Algorithm, we turn to the problem of maximizing sector utilities.

C. Sector Utility Maximization

Let \mathcal{F} denote the (finite) set of fading states $l \in \mathcal{F}$ (reported by mobile terminals), which is not controllable. Moreover let $\mathcal{S}(l)$ be the (finite) set of possible scheduling decisions $s \in \mathcal{S}(l)$, given fading state l .

Then, the problem to solve in sector m is

$$\begin{aligned} & \max_{\bar{X}^m} \sum_i U^m(\bar{X}_i^m) \quad (2) \\ & \text{s.t. } \bar{X}^m \leq \sum_l \pi(l) \sum_j \sum_{s \in \mathcal{S}(l)} \phi_{js}^{lm} \sum_b \mu_{jb}^l(s) \\ & 1 = \sum_s \phi_{js}^{lm} \text{ all } l, j, m \\ & 0 \leq \phi_{js}^{lm} \leq 1 \end{aligned}$$

with $\pi(l)$ being the probability of fading state l (with $\sum_l \pi(l) = 1$) and ϕ_{js}^{lm} being the long term time-fractions of decision s being chosen on PRB j within sector m given state l . Thereby $\mu_{jb}^l(s) = (\mu_{jb1}^l(s), \dots, \mu_{jbI_m}^l(s))$ is the vector of user rates on beam b and PRB j , associated with scheduling decision s .

Gradient Scheduler: In order to solve Problem (2), a standard gradient scheduler is used. With fading-state $l(t)$ given, the gradient scheduler independently solves for each PRB j :

$$s^*(t) \in \arg \max_{s \in \mathcal{S}(l)} \nabla U^m(\bar{X}(t)) \sum_b \mu_{jb}^{l(t)}(s), \quad (3)$$

and updates the average user rates as follows:

$$\bar{X}(t+1) = (1 - \beta) J \bar{X}(t) + \beta \sum_b \mu_{jb}^{l(t)}(s^*(t)).$$

Thereby parameter $\beta > 0$ is small and fixed.

From [8] we know that for $\beta \rightarrow 0$ the gradient scheduling algorithm asymptotically solves Problem (2) without having to know the fading distribution π .

One example of above described gradient scheduler is an approximation of the proportional fair scheduler, which we use as baseline for our performance evaluations and which is explained in greater detail in Section IV-C. The scheduler obtains short-term channel state information (CSI) in the form of channel directional information (CDI) and channel quality information (CQI). The former is just the index of the best beam, while the latter is an SINR estimate in case the user was scheduled exclusively and on its favourite beam. Given fading state $l(t)$, the set of possible scheduling decisions $\mathcal{S}(l)$ is now determined by the following rules: To each user power can be allocated solely on its best beam (determined by the CDI). Once a beam is selected neighboring beams (up to a predefined beam-distance) are “blocked”.

In our proposed (VSA) algorithm, the (gradient) scheduler assigns each potential resource (i.e. beam) a user based upon short-term CSI and e.g. the proportional fair criterion. Due to our assumption that beams (and PRBs, naturally) are never switched off (powers can be arbitrarily low¹ though!) scheduling turns out to be particularly easy since *it works beam-wise circumventing complicated combinatorial beam selection problems*.

II. VIRTUAL SUBBAND ALGORITHM (VSA)

A. Communication Protocol

The general procedure is depicted in Figure 2.

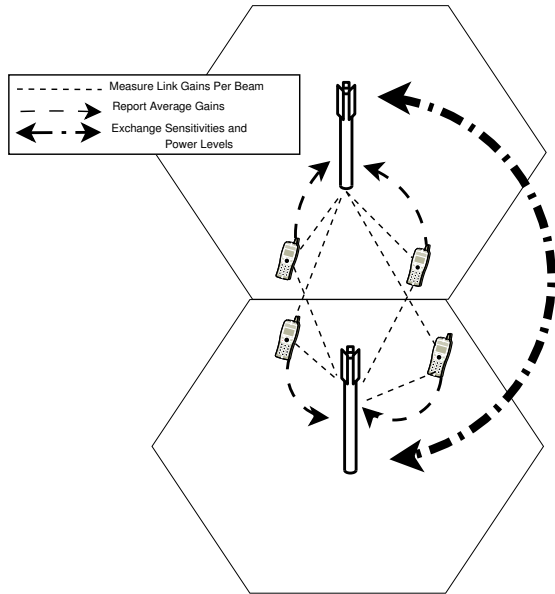


Fig. 2. General Communication Protocol.

In addition to ordinary *short-term CSI*, the mobiles measure and average (subject to control power of pilots) their link

¹From a user’s perspective a beam can of course *appear* to be switched off due to arbitrary low power, however from a scheduling perspective it is still “on”.

gains per beam to all sector controllers. Averaging is done to suppress the effects of fast fading. We define

$$G_{ijb}^m = \overline{|\langle h_{ij}^m, u_b \rangle|^2} \quad (4)$$

to be the average² link gain of mobile terminal i on beam b and PRB j to sector controller m . The gains are reported back to the serving sector controller from time to time (on a lower rate compared to short-term CSI), thus representing *long-term CSI*.

Based on the incoming long-term CSI, the sector controllers can (re-)calculate sensitivities to power changes on particular beams in other sectors (and in the own sector). This information is compiled in messages which are exchanged between the sectors (thus, each sector sends a vector of JB real values to all other sectors³). Upon reception of the message vectors, the sector controllers can calculate an estimate of the *system* utility’s sensitivity to power changes on particular beams and adjust powers accordingly.

In addition to sensitivities, information about transmit powers has to be exchanged between sector controllers on the same time scale as long-term CSI is reported.

B. Virtual Model

The general procedure can be viewed as a generalization of the MGR algorithm in [6] to a network employing beamforming. For the ease of notation we will omit the time index t from now on. However note, that the virtual control actions described below do not have to be performed in each TTI, but only when an update of long-terminal CSI is available.

Given long-term CSI the base station calculates corresponding virtual rates according to

$$R_{ijb}^k =: \rho(F_{ijb}^k), \quad \text{with} \\ F_{ijb}^k = \frac{G_{ijb}^k P_{jb}^k}{\sigma^2 + \sum_{b' \neq b} G_{ijb'}^k P_{jb'}^k + \sum_{m \neq k} \sum_{b''} P_{jb''}^m G_{ijb''}^m}.$$

Here, G_{ijb}^k denote the average link gains defined in Eq. (4). Furthermore, we use Shannon rates $\rho(x) = \log(1+x)$. Note, that F_{ijb}^k can be viewed as a virtual, or long-term, SINR where both adjacent beams b' in sector k , and beams b'' from all other sectors $m \neq k$ are treated as possible sources of interference. Again, since all beams are in use in all sectors, the mobile terminal needs no knowledge about scheduling decisions. In turn, the information about actual beam powers needs to be exchanged between neighboring sectors.

Since all rates are now connected through the virtual model we can calculate sensitivities of a change of P_{jb}^m in sector m on sector k ’s utility defined as

$$D_{jb}^{m,k} := \frac{\partial U^k(X^k)}{\partial P_{jb}^m} \quad (5)$$

²The bar denotes empirical averaging over time.

³To reduce messaging overhead, sector controllers could limit the message exchange to strongest interferers, e.g. consider only neighbouring base stations.

(including $D_{jb}^{k,k}$!) with respect to virtual rates of user i in sector k given by

$$X_i^k = \sum_{j=1}^J \sum_{b=1}^N \tilde{\phi}_{ijb}^k R_{ijb}^k. \quad (6)$$

The parameters $\tilde{\phi}_{ijb}^k$ represent the optimal (for fixed control parameters, i.e. powers) time fractions of resource usage in the virtual model and are generated through virtual scheduling described below.

C. Virtual Scheduling

In order to calculate the time-fraction parameters $\tilde{\phi}_{ijb}^k$ and the sensitivities $D_{jb}^{m,k}$ respectively we use virtual scheduling. However, since the resources are no longer orthogonal but interfere with each other we can no longer employ a scheme as described in [6].

Recall the definition of virtual average user rates X_i^k , defined in (6). In order to generate the optimal parameters $\tilde{\phi}_{ijb}^k$ the virtual scheduler has to solve the following problem⁴ (the same utility as in Eq. (1) must be applied.):

$$f(R) := \max_{\phi_{ijb}^k} \sum_i U^k \left(\sum_j \sum_b \phi_{ijb}^k R_{ijb}^k \right) \quad (7)$$

s.t. $\sum_i \phi_{ijb}^k = 1, \quad 0 \leq \phi_{ijb}^k \leq 1,$

It is important to note that the function $f(R)$ is not necessarily differentiable as it would be necessary for the calculation of sensitivities in (5). However, in Theorem 1 (in Section III) we establish a function family $f_\varepsilon(R)$ (defined by (10)) which is differentiable and “close” to f in a suitable sense. Replacing the original problem with the new one yields then well defined partial derivatives. Please note that this is more than just a side note as it establishes at least convergence of a gradient ascent algorithm to a local maximum.

With reference to the results of Section III we will now write the expressions for the partial derivatives of function $f_\varepsilon(R)$, as opposed to $f(R)$. (The virtual scheduling of [6] can be modified accordingly, if it is used.) We have:

$$D_{jb}^{m,k} = \sum_i \frac{\partial U^k}{\partial X_i^k} \frac{\partial X_i^k}{\partial P_{jb}^m} = \sum_i \frac{\partial U^k}{\partial X_i^k} \sum_{b'} \left(\tilde{\phi}_{ijb'}^k \right)^{1-\varepsilon} \frac{\partial R_{ijb'}^k}{\partial P_{jb}^m} \quad (8)$$

where

$$\frac{\partial R_{ijb'}^k}{\partial P_{jb}^m} = \begin{cases} \rho' \left(F_{ijb'}^k \right) \frac{F_{ijb'}^k}{P_{jb}^m} & m = k, b' = b \\ -\rho' \left(F_{ijb'}^k \right) \frac{(F_{ijb'}^k)^2}{P_{jb}^k} \frac{G_{ijb}^k}{G_{ijb'}^k} & m = k, b' \neq b \\ -\rho' \left(F_{ijb'}^k \right) \frac{(F_{ijb'}^k)^2}{P_{jb}^k} \frac{G_{ijb}^m}{G_{ijb'}^k} & m \neq k \end{cases}$$

The such generated sensitivities are exchanged from time to time between all sector controllers. Thereby every sector k

receives $J \cdot B$ sensitivity values from all other $(M-1)$ sectors, in addition to the $J \cdot B$ values from its own sector. Thus we have

$$D_{jb}^k = \sum_{m=1}^M D_{jb}^{k,m}, \quad (9)$$

summing up the sensitivities of all sectors (including itself) to a power change of beam b on PRB j in sector k and which can be either positive or negative. Note, that sector indices k and m in the RHS of (9) are interchanged compared with (8), since in (8) we are interested in how the beam in sector m interferes with sector k while in (9) it is of interest how the beam in sector k interferes with (all) sector(s) m .

Clearly, since $D_{jb}^{k,m}$ represent estimates of the sector utilities to a power change on jb in sector k , D_{jb}^k is an estimate of the *system's* utility to a power change on the respective beam. Depending on the D_{jb}^k we can now make a power adjustment which steers the system operating point towards a greater utility in the virtual model.

D. Power Control

The power adjustment is carried out in steps of $\Delta > 0$, which is small and fixed. Let $\bar{P}^k(t)$ denote the current total allocated power in sector k and P^* the upper bound on the total sector powers.

- 1) Pick a virtual resource $(jb)_*$ (if there is one) such that $D_{(jb)_*}^{(k)}(t)$ is the smallest among all virtual resources jb with $D_{jb}^{(k)}(t) < 0$ and $P_{jb}^k(t) > 0$. Now, set

$$P_{(jb)_*}^k(t+1) = \max \left\{ P_{(jb)_*}^k(t) - \Delta, 0 \right\}.$$

- 2) If $\bar{P}^k(t) < P^*$, pick $(jb)_*$ (if there is one) such that $D_{(jb)_*}^{(k)}(t)$ is the largest among those jb with $D_{jb}^{(k)}(t) > 0$. Set

$$P_{(jb)_*}^k(t+1) = P_{(jb)_*}^k(t) + \min \left\{ \Delta, P^* - \bar{P}^k(t) \right\}.$$

- 3) If $\bar{P}^k(t) = P^*$ and $\max_{jb} D_{jb}^{(k)}(t) > 0$, pick a pair $((jb)_*, (jb)^*)$ (if there is one) such that $D_{(jb)_*}^{(k)}(t)$ is the largest, and $D_{(jb)^*}^{(k)}(t)$ is the smallest among those virtual resources jb with $P_{jb}^k(t) > 0$ and $D_{(jb)^*}^{(k)}(t) < D_{(jb)_*}^{(k)}(t)$. Set

$$P_{(jb)_*}^k(t+1) = \max \left\{ P_{(jb)_*}^k(t) - \Delta, 0 \right\}, \quad \text{and}$$

$$P_{(jb)^*}^k(t+1) = P_{(jb)^*}^k(t) + \min \left\{ \Delta, P_{(jb)^*}^k(t) \right\}.$$

Note, that for practical purposes it may be necessary to specify a certain minimum power per beam P_b^{\min} instead of allowing beam powers to be reduced to zero. In this case the changes to the algorithmic notation above are straight forward, so we do not explicitly state them here.

By intuition, the algorithm reallocates power to the beams with large positive utility-sensitivity.

⁴We collected all rates R_{ijb}^k in R .

III. SOME RELATED THEORETICAL RESULTS

As mentioned before, the problem to solve for every sector controller is given in (7). Let us define a slightly modified version

$$f_\varepsilon(R) := \max_{\phi_{ijb}^m} \sum_i U^m \left(\sum_j \sum_b (\phi_{ijb}^m)^{1-\varepsilon} R_{ijb}^m \right). \quad (10)$$

One can show the following:

Theorem 1. *Let $0 < \varepsilon < 1$ be finite and U^m be an increasing concave utility function, defined in $(0, \infty)$. Then, the family of functions $f_\varepsilon(R)$ (defined by (10)) with $R_{ijb} \geq c > 0$ ($\forall i, j, b$) is differentiable everywhere and converges for any sequence $\varepsilon_n \rightarrow 0$ to f in (7) (which is continuous) in the uniform sense.*

Proof: First we show that $f_\varepsilon(R)$ is everywhere differentiable. For this purpose we use the following Lemma 2 and set $H(x, y) := U(R, \Phi)$.

Lemma 2. *Consider a function $H(x, y)$, $x \in [a_1, a_2]$, $y \in [a_3, a_4]$, with some finite $a_1 < a_2$ and $a_3 < a_4$. Assume that $H(x, y)$ and its partial derivative on x are continuous, and $H(x, y)$ is concave in x (for each y) and strictly concave in y (for each x). Then the function*

$$\varphi(x) = \max_y H(x, y) \quad (11)$$

is continuously differentiable in $[a_1, a_2]$. (This can be generalized to the multi-dimensional case. Namely the domains $[a_1, a_2]$ and $[a_3, a_4]$ can be replaced by arbitrary convex compact sets in finite-dimensional vector spaces, and derivatives replaced by gradients.)

Note that Lemma 2 cannot be applied directly to (7) since concavity in y is in this case not given.

Clearly R and Φ are compact since $\phi_{ijb} \in [0, 1]$ and $R_{ijb} \in [c, B]$, $B < \infty, c > 0$. Moreover, the concavity of U follows by definition. Now we have to show that $f_\varepsilon(R)$ converges for any zero sequence $\varepsilon_n \rightarrow 0$ to f . First fix a zero sequence ε_n^* . Moreover, we define a sequence of functions

$$f_n(R) := \max_{\phi_{ijb}^m} \sum_i U^m \left(\sum_j \sum_b (\phi_{ijb}^m)^{1-\varepsilon_n^*} R_{ijb}^m \right) = f_{\varepsilon_n^*}(R),$$

with $(n \in \mathbb{N})$. We can use Dini's Theorem to show that $\{f_n(R)\}_{n \in \mathbb{N}}$ converges uniformly to f . This theorem says that if $\{f_n\}_{n \in \mathbb{N}}$ ($f_n : K \rightarrow \mathbb{R}, n \in \mathbb{N}$, being a sequence of continuous functions and K being a compact metric space) converges pointwise to f ($f : K \rightarrow \mathbb{R}$ being a continuous function) and if $f_n(x) \geq f_{n+1}(x)$ ($\forall x \in K$ and $\forall n \in \mathbb{N}$) then $\{f_n\}_{n \in \mathbb{N}}$ converges uniformly to f .

The rate-space $K := [c, B]^{IJJN}$ is clearly compact, since $R_{ijb} \in [c, B]$, $B < \infty, c > 0$. Moreover for each $x^* \in K$, $f_n(x^*)$ converges to $f(x^*)$ when $n \rightarrow \infty$ (since $\varepsilon_n \rightarrow 0$) and since $\phi_{ijb} \in [0, 1]$, we have $\phi^{1-\varepsilon_n} \geq \phi^{1-\varepsilon_m}$ ($\forall i, j, b$) if $m \geq n$. Thus $f_n(x) \geq f_{n+1}(x)$. \square

Hence by above theorem, we can replace our utility function with a smooth, uniformly convergent approximation, which can be locally maximized in the power control loop. Please note, that this replacement is already incorporated in the calculation of sensitivities (Eq. (8)).

IV. SIMULATIONS

A. Simulation Setup

To evaluate the performance of VSA we conduct system level simulations. The general simulation setup can be found in Table I. We employ a grid of 7 hexagonal cells each comprising 3 sectors (to ensure equal interference conditions for each sector, a wrap-around model is used at the system borders).

TABLE I
GENERAL SIMULATION SETUP

Parameter	Value
Number of Sectors (M)	21
Total Number of Mobile Terminals (I)	210
Mobile Terminal Velocity	0 km/h, 3 km/h
Number of PRBs (J)	4
Number of Beams (B) (VSA)	4
Number of Beams (B) (Baseline)	8
Minimum Beam-Distance (Baseline)	3
Number of Basestation Antennas (N_{tx})	4
Number of Mobile Terminal Antennas (N_{rx})	1
Simulation Duration	10000 TTI
Power-Control Δ	0.5% of initial power

Note that the users are distributed randomly over the whole area. Although we have an average of 10 users per sector, some sectors have a higher load than others. A detailed description of the used transmit codebook can be found in [7]. As traffic model we use full buffer, that is, we assume there is always data available to transmit to each of the users. As channel model, we use the WINNER model (WiM) ([9]), Scenario C2.

Link Adaptation: All simulations are performed with realistic link adaptation. After resource allocation, each scheduler chooses the modulation and coding scheme (MCS) for each user based on its feedback (CQI) on the acquired resources. Thereby the particular MCS is chosen, which gets closest to a desired block error rate (we use 30%). For it, curves are available for each MCS that map an effective SINR to a block error rate. The effective SINR is thereby determined through MIESM (mutual information effective SINR mapping) of the CQI values of all resources the user is scheduled on.

In the simulations, there is an explicit modelling of HARQ (hybrid automatic repeat request) using Chase combining. In case of an error (e.g. in case the MCS was chosen too optimistically) the whole transmission of a user has to be retransmitted. Thereby HARQ-users with a pending retransmission are prioritized over non-HARQ users.

B. VSA Configuration

In VSA we have to distinguish between feedback for the actual scheduler and feedback for the virtual scheduler. The actual scheduler receives for each codebook entry a CQI value, which represents the SINR if the user was scheduled on the respective beam. The SINR is accurate (except a delay of 1 TTI) because the mobile is able to determine the real interference situation (since all beams are always turned on, and the power levels P_{jb}^k are assumed to be known to the mobile for all j , b , and k).

The 'virtual' feedback consists of the average link gains G_{ijb}^k defined in Eq. (4). The link gains are exponentially averaged with an averaging factor of $\beta = 0.0034$. In our simulations they are reported accurately, that is, without quantization. All feedback is reported on a per-TTI basis.

Since every beam on every PRB is used, we have in total $N \cdot J$ resources available for scheduling. The scheduler chooses for each beam and each PRB the best user, w.r.t. the gradient algorithm (see Eq. (3)).

We start with an equal power allocation to each virtual resource, that is, $P_{jb}^m(0) = \frac{P^*}{J \cdot N}$ (with P^* being the total power available). The power control step Δ is set to 0.5 percent of the initial beam power P_{jb}^m .

C. Baseline Algorithm Configuration

As baseline we use the simple non-coordinative GBD algorithm, with a codebook size of 3 bit (8 beams). As already introduced in Section I-C, GBD requires for each user feedback comprising a CDI and a CQI value. Note, the CQI is only an estimate of the user's SINR, since the scheduling decisions cannot be known in advance. Thus, it does not contain intra-sector interference; the user is assumed to be scheduled on the PRB alone (with full power). Moreover it contains only an estimate of the inter-sector interference.

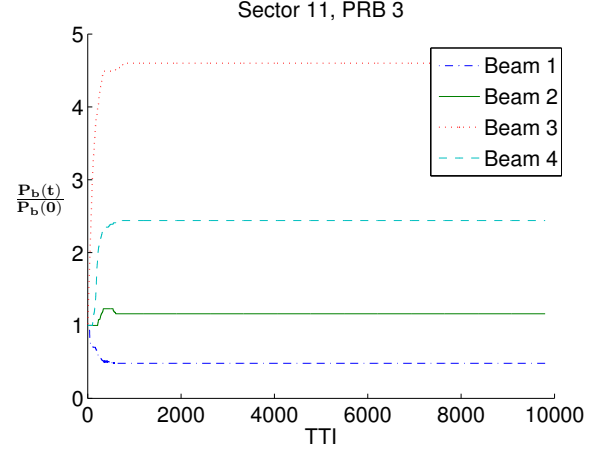
On each PRB the users are greedily scheduled on their best beams (using their proportionally fair weighted CQI-feedback as utility). Thereby a minimum beam-distance has to be kept, in order to minimize the interference between users scheduled on the same PRB. This distance is based on a geometrical interpretation of the beamforming as in Figure 1. It means that given a user is scheduled on a certain beam, adjacent beams (up to a certain 'distance') are blocked and users that reported one of those beams are excluded from the list of scheduling candidates for the respective PRB. We use a minimum distance of 3, that is, with the used 8-beam codebook at most 3 users can be scheduled on the same PRB.

Of course, no adaptive power allocation is performed, the power is distributed equally among the PRBs (and further among the thereon scheduled users).

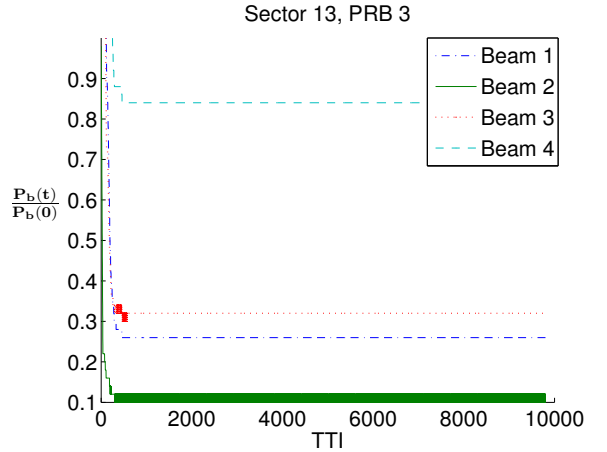
D. Results in a static setting

1) *Power Control*: First, we show that VSA indeed creates a power distribution between both beams and PRBs. Figure 3 depicts results for 2 different sectors, showing beam powers on a selected PRB, normalized to the original beam power over time (that is, $\forall b$ and j fixed: $\frac{P_{jb}(t)}{P_{jb}(0)}$). As expected, it turns out

that some beams are run with very high power (e.g. beam 3 in 3(a)) while others are almost shut down (e.g. beam 2 in 3(b)).



(a) Example 1



(b) Example 2

Fig. 3. Examples of power spread across beams

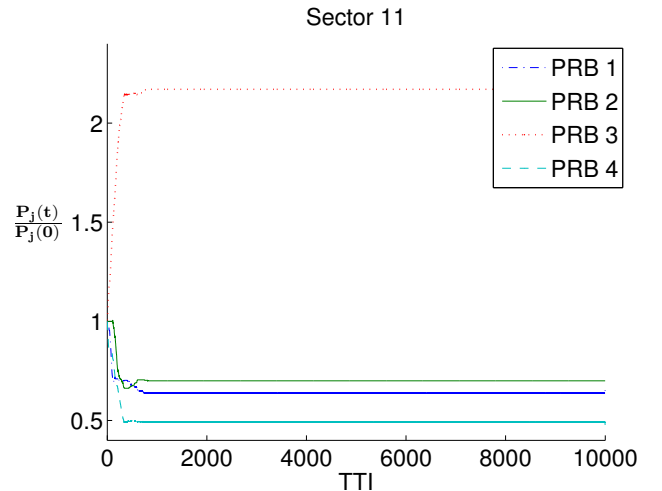


Fig. 4. Example of power spread across PRBs.

In addition, VSA produces some soft fractional frequency reuse by allocating different power levels to different subbands. An example of this is depicted in Figure 4. The term “soft” means an unequal power allocation to PRBs in order to reduce interference, as opposed to a hard reuse which would completely shutdown subbands, thus eliminating interference but wasting resources. In this respect VSA clearly differs from the baseline GBD algorithm which cannot create a power spread across PRBs.

2) *Geometric Average of User Throughputs*: Since the utility functions are the sum of logarithmic user throughputs, we use the geometric mean of user throughputs (GAT) as performance metric in our comparisons. More precisely we look at the average cumulated user throughput, that is, at time T we sum up the throughputs of each user from TTI 1 to TTI T . Thus

$$GAT = \exp \left(\frac{1}{I} \sum_i \log \left(\frac{1}{T} \sum_{t=1}^T R_i(t) \right) \right),$$

with $R_i(t)$ being the throughput of user i in TTI t . Figure 5 compares the GAT of VSA and GBD, showing a significant gain of VSA over GBD (of about 23%). The somehow peculiar behaviour of the curves, being zero first and after a while immediately taking a non-zero value, can be explained with the logarithmic nature of the GAT, which cannot be calculated while there is at least one user who did not receive any resources yet.

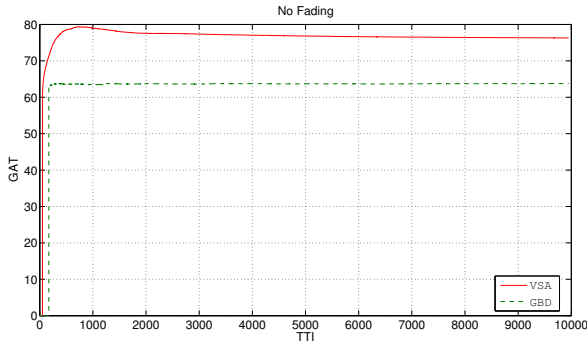


Fig. 5. Performance gain of Virtual Subband Algorithm over GBD Scheduling

3) *Performance of Cell-Edge Users*: The most important criterion for a multi-cell coordinative scheduling scheme as VSA, however, is the performance of cell-edge users. As a measure for it, we look at the 5%-quantile of the average user throughputs of all users in the system. Similar to the calculation of GAT we plot the 5-percentile of the normalized cumulated user throughputs at each TTI. As shown in Figure 6, the gain of VSA improves even further (more than 200%) when looking at cell-edge users only.

E. Results in a fast-fading setting

The situation somewhat changes when we permit fast-fading channels. Here we assume the mobile terminals move with

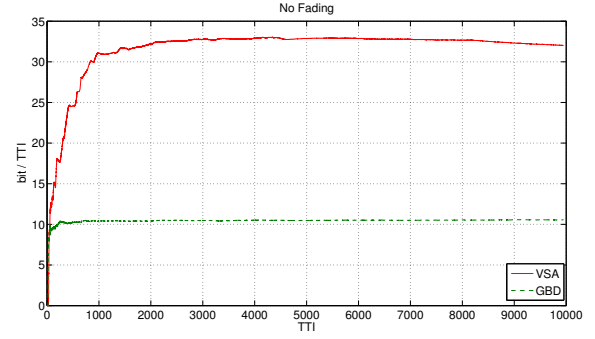


Fig. 6. Performance gain of cell-edge users

a velocity of 3 km/h. Figure 7 depicts the comparison of VSA and GBD w.r.t. GAT for the fast-fading case. Here we experience a decrease in utility (about 11%). We will discuss the reasons for this below. However when looking at the performance of cell-edge users we still benefit from coordination. As depicted in Figure 8 in the end we still have a gain more than 20% in the 5%-user throughput of VSA over GBD.

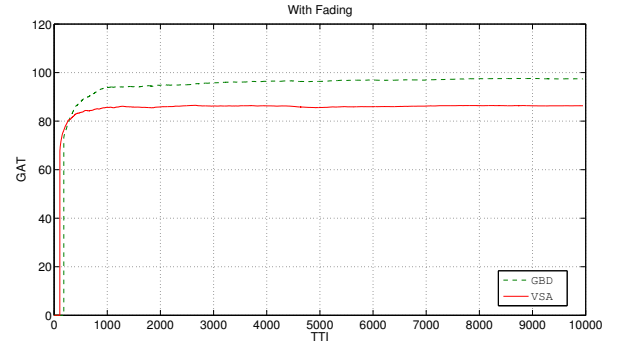


Fig. 7. Performance gain of Virtual Subband Algorithm over GBD Scheduling

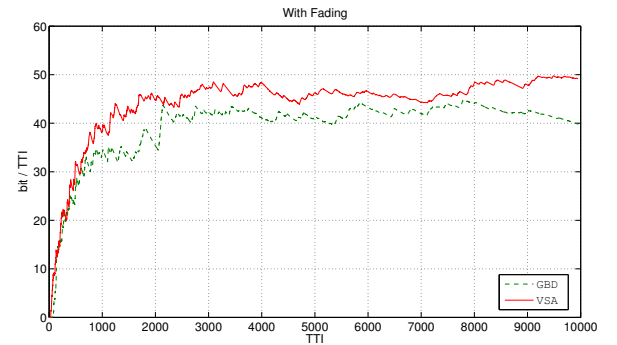


Fig. 8. Performance gain of cell-edge users

We think the reasons for the decrease in performance

in the presence of fast-fading can be reduced to a “model mismatch” between the virtual model and the “real” system which experiences strongly varying channels. In such a setting the highly opportunistic GBD algorithm can much better react to the instantaneous fading situation (including completely shutting down beams for a short time period) than VSA which performs long-term power control based on the virtual model.

V. CONCLUSION AND FUTURE WORK

We presented an algorithm—called VSA—for distributed interference coordination in a cellular network with OFDM and spatial beamforming. The algorithm relies on a grid of fixed, always switched-on beams and adapts transmit powers on a per-beam granularity, minimizing both inter- and intra-cell interference. Utility maximization through power control is based on an exchange of messages between sector controllers which are calculated based on a virtual model. This model captures the complicated interference situation in the network by linking average user rates through long-term control parameters (transmit powers per beam).

To evaluate the performance we carry out system-level simulations, which show that in a static setting VSA leads to extraordinary gains over a non-cooperative fixed-beams scheduling scheme, both in utility and in particular in the performance of cell-edge users. In a fast-fading environment however, simulations show that a gain in utility cannot always be guaranteed, however we still see a benefit for cell-edge users.

A natural and important further development of the proposed algorithm would be to improve the virtual model in a way to better accommodate to a fast fading environment. First investigations of a more opportunistic control scheme are already carried out and show promising results in this direction. Simulation results indicate that when instantaneously allowing deviations from the strict per-beam power budget, we can expect significant gains even in the fading case. This will be published elsewhere.

REFERENCES

- [1] D. Gesbert, S. Kiani, A. Gjendemsj, and G. ien, “Adaptation, coordination, and distributed resource allocation in interference-limited wireless networks,” *Proceedings of the IEEE*, vol. 95, no. 12, pp. 2393–2409, Dec. 2007.
- [2] O. Somekh, O. Simeone, Y. Bar-Ness, A. M. Haimovich, and S. Shamai, “Cooperative multicell zero-forcing beamforming in cellular downlink channels,” *IEEE T Inform Theory*, vol. 55, no. 7, pp. 3206–3219, Jul. 2009.
- [3] W. Choi and J. Andrews, “The capacity gain from intercell scheduling in multi-antenna systems,” *Wireless Communications, IEEE Transactions on*, vol. 7, no. 2, pp. 714–725, February 2008.
- [4] H. J. Bang and D. Gesbert, “Multicell zero-forcing and user scheduling on the downlink of a linear cell array,” Nov. 2009. [Online]. Available: <http://arxiv.org/abs/0911.0971>
- [5] R. Bhagavatula and R. W. H. Jr., “Adaptive limited feedback for sum-rate maximizing beamforming in cooperative multicell systems,” Dec. 2009. [Online]. Available: <http://arxiv.org/abs/0912.0962>
- [6] A. L. Stolyar and H. Viswanathan, “Self-organizing dynamic fractional frequency reuse for best-effort traffic through distributed inter-cell coordination,” in *Proceeding of INFOCOM*, 2009.
- [7] 3GPP R1-073937, Alcatel-Lucent, “Comparison aspects of fixed and adaptive beamforming for LTE downlink,” 3GPP TSG RAN WG1 #50bis Shanghai, China, October 8 – 12, 2007.
- [8] A. L. Stolyar, “On the asymptotic optimality of the gradient scheduling algorithm for multiuser throughput allocation,” *Operations Research*, vol. 1, pp. 12–25, 2005.
- [9] “D5.4 final report on link and system level channel models,” IST-2003-507581 WINNER, Tech. Rep., 2005.